Transcranial Magnetic Stimulation Over the Human Medial Posterior Parietal Cortex Disrupts Depth Encoding During Reach Planning

CEREBRAL CORTEX

Transcranial magnetic stimulation over the human medial posterior parietal cortex disrupts depth encoding during reach planning.

Rossella Breveglieri[1]*, Annalisa Bosco[1°], Sara Borgomaneri[2,3°], Alessia Tessari[5], Claudio Galletti[1], Alessio Avenanti[2,4], Patrizia Fattori[1].

1. Department of Biomedical and Neuromotor Sciences, University of Bologna, 40126 Bologna, Italy

2. Center for studies and research in Cognitive Neuroscience, University of Bologna, 47521 Cesena, Italy.

3. IRCCS Santa Lucia Foundation, 00179 Rome, Italy.

4. Center for research in Neuropsychology and Cognitive Neurosciences, Catholic University of Maule, 3460000 Talca, Chile.

5. Department of Psychology, University of Bologna, 40127 Bologna, Italy

° these authors have contributed equally.

***Corresponding author**

Prof. Rossella Breveglieri

Department of Biomedical and Neuromotor Sciences, University of Bologna, Piazza di Porta S. Donato 2, 40126, Bologna, Italy

Phone: 00390512091890

Fax: 00390512091737

Email: rossella.breveglieri@unibo.it

Running title:

TMS over hV6A disrupts depth encoding of reaching plans

Abstract

Accumulating evidence supports the view that the medial part of the posterior parietal cortex (mPPC) is involved in the planning of reaching, but while plenty of studies investigated reaching performed towards different directions, only a few studied different depths. Here, we investigated the causal role of mPPC (putatively, human area V6A - hV6A) in encoding depth and direction of reaching. Specifically, we applied single-pulse transcranial magnetic stimulation (TMS) over the left hV6A at different time points while 15 participants were planning immediate, visually-guided reaching by using different eye-hand configurations. We found that TMS delivered over hV6A 200 ms after the Go signal affected the encoding of the depth of reaching by decreasing the accuracy of movements towards targets located farther with respect to the gazed position, but only when they were also far from the body. The effectiveness of both retinotopic (farther with respect to the gaze) and spatial position (far from the body) is in agreement with the presence in the monkey V6A of neurons employing either retinotopic, spatial, or mixed reference frames during reach plan. This work provides the first causal evidence of the critical role of hV6A in the planning of visually-guided reaching movements in depth.

Keywords

Human V6A, transcranial magnetic stimulation, reaching in depth, reach plan, eye-hand configuration

In humans and monkeys, the medial posterior parietal cortex (PPC) has a major role in monitoring and guiding reaching movements (Cavina-Pratesi, Monaco, et al. 2010)(Goodale and Milner 1992)(Jeannerod et al. 1995)(Andersen et al. 1997)(Colby and Goldberg 1999)(Fattori et al. 2017)(Filimon 2010)(Culham and Valyear 2006; Culham et al. 2006). Studies on patients revealed that PPC lesions lead to a neurological condition called optic ataxia, which results in incorrect reaching movements towards targets located in peripheral vision, whereas normal reaching towards foveated targets are correctly performed (Perenin and Vighetto 1983; Karnath and Perenin 2005)(Perenin and Vighetto 1988)(Blangero et al. 2009)(Rossetti et al. 2005)(Vallar and Branch Coslett 2018).

In the monkey, the medial part of the PPC hosts area V6A (Galletti et al. 1999)(Gamberini et al. 2011), whose neurons are modulated by reaching movements towards foveated as well as peripheral targets (Bosco et al. 2015)(Fattori et al. 2001, 2005)(Marzocchi et al. 2008)(Bosco et al. 2016)(Fattori et al. 2017). Recent electrophysiological works highlighted the modulating effect of both direction and depth (i.e., amplitude) of reaching movements on V6A neurons (Hadjidimitrakis, Bertozzi, Breveglieri, Bosco, et al. 2014). A lesion study on macaque monkeys showed that, when V6A was surgically removed, the animals showed misgrasping and hypometric misreaching (Battaglini et al. 2002), particularly evident when reaching was directed towards targets located far from the animal (Galletti et al. 2003).

In humans, the cortical lesion of optic ataxia patients is centered in the medial parieto-occipital cortex (Karnath and Perenin 2005), a region which likely involves the human homologous of macaque area V6A (hV6A) (Pitzalis et al. 2015)(Tosoni et al. 2015)(Pitzalis et al. 2013). Some patients with lesions in the PPC show more significant visuomotor deficits in depth than in direction, which lead to a specific impairment of arm movements toward targets arranged at different distances from their body (Holmes and Horrax 1919; Baylis and Baylis 2001; Danckert et al. 2009). However, as human studies typically involve large lesions, it is difficult to correlate a specific deficit with a single cortical area and, conversely, no human patient with a lesion restricted to the hV6A has been studied to date.

Transcranial magnetic stimulation (TMS) represents a unique opportunity to fill this gap of knowledge because it allows to reversibly perturb restricted, selected brain regions on the cortical surface and to test their causal role on behavior (Pascual-Leone et al. 1999). The TMS studies involving the medial PPC (mPPC) conducted so far (Ciavarro et al. 2013)(Dessing et al. 2013; Vesia et al. 2017)(Vesia et al. 2010, 2013) demonstrated a specific involvement of the mPPC in encoding peripheral reaching. Specifically, Vesia and coworkers (Vesia et al. 2010) and Ciavarro and coworkers (Ciavarro et al. 2013) showed that a train of repetitive TMS applied over the mPPC during reach planning caused a deviation of memorized reaching endpoint towards the position of visual fixation (misreaching) that resembled optic ataxia deficits. However, the repetitive TMS paradigm prevented the possibility to investigate the timing of the mPPC involvement. Even more importantly, as participants in these prior studies only performed peripheral reaching and reaches to targets located at different depths were not tested, it remains speculative whether the human mPPC plays causal roles in guiding the arm towards foveated targets and specifically at different depths.

Thus, to address these questions, we investigated the causal role of human mPPC (putatively hV6A according to (Pitzalis et al. 2013)(Tosoni et al. 2015)(Ciavarro et al. 2013)) in the encoding of depth and direction of reaching movements in different eye-hand configurations (foveal and peripheral reaching). To this aim, we used single-pulse TMS (spTMS) administered at two time-points during the reaction time (planning phase before the movement onset) of an immediate, visually-guided reaching task.

Materials and Methods

Participants.

Fifteen healthy volunteers (three males and twelve females; age range 20-29 years; mean age 22.6+/-2.49 years) participated in this study. The number of participants has been determined basing on a power analysis, that indicated that a sample size of 15 participants is necessary to achieve a statistical

power (1 – β) of 0.90 (2-tailed α = 0.05; effect size f = 0.20; number of measurements = 18; correlation = 0.6, analysis performed with G*Power software (Faul et al. 2007).

All the participants were right-handed according to a standard handedness inventory (Briggs and Nebes, 1975), had normal or corrected-to-normal visual acuity in both eyes, and were naïve as to the purposes of the experiment. None of the participants had neurological, psychiatric, or other medical problems or any contraindication to TMS (Rossi et al., 2009). Participants provided written informed consent, and the procedures were approved by the Bioethical Committee at the University of Bologna (Prot. 170133, 21st Nov 2018) and were in accordance with the ethical standards of the 2013 Declaration of Helsinki. No discomfort or adverse effects during TMS were reported or noticed.

Localization of brain sites.

To identify the target area hV6A, we used frameless stereotaxic neuronavigation. Before each experimental session, the coil position was identified on each participant's scalp wearing a bathing cap using the SofTaxic Navigator system (EMS, Bologna, Italy) (Carducci and Brusco 2012)(Valchev et al. 2017)(Avenanti et al. 2018). In a first step, skull landmarks (nasion, inion, and 2 preauricular points) and 65 points providing a uniform representation of the scalp were digitized by means of a Polaris Vicra Optical Tracking System (Northern Digital, Inc., Waterloo, ON, Canada). Coordinates in Talairach space were automatically estimated by the SofTaxic Navigator from an MRI-constructed stereotaxic template. This procedure has been proven to ensure a good localization accuracy, showing an error of roughly 5 mm in comparison to methods based on individual MRIs (Carducci and Brusco 2012).

The Talairach coordinates we used were x = −10, y = –78, z = 40 (Fig. 1A) (Talairach and Tournoux 1988). These coordinates are the same as used in a previous TMS study on hV6A (Ciavarro et al. 2013), and are similar to those used for studying the SPOC (Superior parieto-occipital cortex) (Vesia et al. 2010, 2013, 2017), a region also investigated in imaging studies (Cavina-Pratesi, Monaco, et al. 2010)(Gallivan et al. 2009, 2011; Monaco et al. 2014)(Rossit et al. 2013) that likely includes hV6A

(Fattori et al. 2017). In each participant, the hV6A scalp sites were marked on the bathing cap with a pen. Then, the neuronavigation system was used to estimate the projections of the scalp sites on the brain surface. Mean coordinates ± standard deviation corresponded to the hV6A (mean x = –10.2 ± 1.3 y = –76.9 ± 2.9 z = 40.6 ± 2.5).

TMS was also applied to the occipital cortex (area V1/V2) to control for the nonspecific effects of the TMS stimulation (Kamitani and Shimojo 1999)(Chiappini et al. 2018). To target V1/V2, the coil was centered 2 cm dorsal to the inion (Romei et al. 2016), holding the handle tangentially to the scalp and pointing downwards (Vesia et al. 2010).

TMS protocol.

Biphasic spTMS was delivered using a MagStim Rapid2 stimulator and a 70 mm figure-of-eight coil. Stimulation of hV6A was carried out by placing the coil tangentially over the marked scalp sites along a parasagittal line with the handle pointing downward (Vesia et al. 2010).

Sham stimulation was performed by placing the coil tilted at 90° over the vertex, so that no current was induced in the brain (Lisanby et al. 2001). As known from previous experiments (Lisanby et al. 2001; Sandrini et al. 2011), by adopting this procedure, no effective magnetic stimulation reached the brain during the sham condition, while the participants' feeling of coil–scalp contact and discharge noise were similar to the real stimulation. We administered sham stimulation over a single site (the vertex) instead of over each of the target areas to provide a single control condition for both hV6A and occipital sites, i.e., avoiding an increase in the number of trials (Jacquet and Avenanti 2015)(Lockwood et al. 2013)(Amemiya et al. 2017)(Paracampo et al. 2018).

To minimize potential TMS after effects on cortical activity that outlast the period of direct stimulation (Pascual-leone et al. 1994; Wang et al. 1996; Levkovitz et al. 1999; Siebner and Rothwell 2003; Siebner et al. 2009) while keeping the duration of the experiment acceptable, the intertrial period of the task (see below) was randomly set at 5-7s. Custom software externally triggered the TMS at reaching target onset, as explained below (see Behavioral task).

The intensity of magnetic stimulation was fixed at 70% of the maximal stimulator output as in Smyrnis et al (Smyrnis et al. 2003) and similar to several previous TMS studies targeting the posterior parietal cortex (Vesia et al. 2010)(Buelte et al., 2008; Dambeck et al., 2006; Lewald et al., 2002; Steven L. Prime et al., 2008; Vesia et al., 2006)(Delle Monache et al. 2017).

None of the participants reported the presence of scotoma in the visual field during and immediately after TMS, nor any undesirable side effects as a result of the stimulation.

Apparatus and behavioral task

We tested the influence of TMS of the hV6A on reaching preparation by using the apparatus used in a recent psychophysical study (Bosco et al. 2017). It consisted of a 19-inch touchscreen (ELO IntelliTouch 1939L) laid horizontally on a desk located at waist level. It contained the targets of reaching movements performed by the participants with their right hand. In all trials, participants started the reaching movement with their right hand on a button (home-button) placed adjacent to the touchscreen in front of the participant's chest, as sketched in Figure 1B. The participants performed immediate (i.e., without delay) reaching movements.

The reaching movements were performed in a darkened room. The head of participants was supported by a chin rest in order to reduce head movements. The stimuli were green (fixation point, diameter 0.3 cm) and red (reaching target, diameter 1.2 cm) dots presented at different depths and in different directions with respect to participant's midline (Fig. 1B). The stimuli had a luminance of about 17 cd/m^2. The visible display size of the touchscreen was 37.5 x 30 cm. It contained 15.500 touch points/cm^2. The display had a resolution of 1152 x 864 pixels and a frame rate of 60 Hz.

Figure 1B shows target positions with respect to the participant's body. There were nine possible locations where targets could appear: three placed at a near distance (18.5 cm from the initial hand position), three at an intermediate distance (30 cm from the initial hand position), and three at a far distance (41.5 cm from the initial hand position, Fig. 1B). The targets were arranged in a square of 23 x 23 cm, and were located 11.5 cm apart from each other, either on the left or the right side; the

central targets were placed along the sagittal midline. All targets were located within a comfortable reaching distance for all participants tested.

The task presented different eye/target configurations (see Fig. 1C): the *Constant gaze configuration*, in which the eye fixated a central fixation target and the hand reached to one of the 8 peripheral reaching targets; the *Constant reach configuration*, in which the eyes fixated one of the 8 peripheral targets and the hand always reached the central target; and *Foveal reach configuration*, in which fixation and reaching targets were coincident. Notice that in both Constant gaze and Constant reach configurations, the position of the fixation point was not coincident with the position of the reaching target, so they were all peripheral reaching.

The sequence of visually guided reaching (Fig. 1D) consisted of an intertrial period (Intertrial) whose duration was randomly chosen between 5, 6 or 7 s, followed by the presentation of the fixation point that prompted the participant to press the home-button. Then, the participant had to stare at the fixation point (Fixation) for a period whose duration was randomly chosen trial by trial (1.3 or 1.5s). After this period, the reaching target appeared (Cue/Go) and this indicated: i) the position to reach; ii) that the participant had to promptly reach that target position while maintaining fixation on the fixation target (immediate reaching).

To investigate the timing of the involvement of hV6A in action planning, we delivered a spTMS at two different timings (100 ms or 200 ms) from target onset (Go signal) in different trials. We selected these two times as they tap early vs. later phases of reach planning, while falling well within participants' reaction time (Table S1). The fixation point and reaching target remained illuminated until the participant completed the arm movement (visually guided reaching). When the participant touched the target on the touchscreen (Movement offset), the target and fixation point switched off and a new intertrial period started.

The task was composed of 30 blocks of 25 trials each (8 trials for Constant gaze condition, 8 for Constant reach condition, 9 for Foveal reach condition) for a total of 750 trials performed over the same experimental session. Each session lasted approximately 3.5 h. Fifteen blocks were composed

of 100-ms trials, and 15 of 200-ms trials. Out of each fifteen blocks of trials, five blocks involved active stimulation of hV6A, five active stimulation of V1/V2, and the remaining five sham stimulation. Within each block, trials of the three configurations were randomized. We also randomized blocks of 100-ms and 200-ms of each stimulation condition (hV6A, V1/V2, Sham). For stimuli presentation and data analysis, we used Matlab (Mathworks, USA) with the Psychophysics toolbox extension (Brainard 1997).

Data analysis and acquisition

The kinematics of reaching movements was recorded using a motion tracking system (VICON motion capture system, 5 M cameras, 1024 x 1024 pixel resolution) by sampling the position of two markers at a frequency of 100 Hz; markers were attached to the wrist (on the scaphoid bone) and the nail of the right index finger (reaching finger). The trajectories of reaching movements of an exemplary participant in the Sham condition during different eye-hand configurations are shown in Fig. S1.

Reaching onset was detected by the release of the home button. Reaching offset was detected by the touch on the touchscreen. We defined the reaction time as the interval between the "Go" signal and movement onset. Movement time was obtained by subtracting the movement onset from the respective movement offset. Participants were asked to move the hand in a ballistic way (without pauses or interruptions), at a fast but comfortable speed, and as accurately as possible.

Eye position was recorded using a camera-based eye-tracker (Pupil Lab, Pupil Labs Gmbh) recording real-time gaze position at 200 Hz. The elevation distance between the eyes of participants and the touchscreen was 27 cm (Fig. 1B). Before collecting data from each participant, the equipment was calibrated using a five-point grid that the participants were asked to fixate steadily.

Movement accuracy and precision were extracted by endpoints recorded by the touchscreen and derived from the parameters of 95% confidence ellipses fit to hand position (end-point) distributions measured at movement offset, as performed in previous studies (Vesia et al. 2006, 2010)(Vesia et al. 2008). Constant error (accuracy) was calculated by taking the signed difference between the

horizontal (horizontal error, here referred to as direction error) and vertical (vertical error, here referred to as depth error) coordinates of the center of movement ellipses and each target location (Fig. 1E). Positive direction errors indicate reach end-points to the right of the target; positive depth errors indicate reach end-points nearer to the body than the target. Variable error (precision) was measured using the area of these ellipses (Fig. 1E). Statistical reliability of differences between mean constant errors, variable error, reaction and movement times were tested using repeated-measures ANOVA and Duncan's post hoc tests. In particular, we performed separate three-way repeated measures ANOVAs, for each eye-target configuration and depth/direction dimensions with the following factors: Stimulation Condition (3 levels: Sham, V1/V2, hV6A), Stimulation Time (2 levels: 100 ms, 200 ms), Depth (3 levels: near, intermediate, far) *or* Direction (3 levels: left space, center and right space).

Analysis of gaze positions during the trials was performed (offline) in order to ensure that participants fixated the fixation point during both reaching execution and preparation. This control was particularly important for trials of the Constant gaze and Constant reach configurations, where the positions of the reaching target and fixation point were incongruent. Trials where gaze fixation was not directed to the fixation point were excluded from the subsequent analysis (percentage of removed trials: ~4%). To do this, we have first checked offline the movies created by the Pupil lab system to exclude trials where the gaze was directed far away from the fixation point. Then, we have also excluded the trials where the coordinates of the gaze positions recorded in the period between target onset and movement end were out of a window that contained the 2 standard deviations of these coordinates (Fisher et al. 2017).

Since our aim was to assess the critical role of the hV6A in planning reaching movements, in the main text we report only main effect or interaction of the Stimulation condition, while other effects have been described in the Supplementary material.

Results

Constant gaze configuration (peripheral reaching)

Reach end-point precision

Reach end-point precision is expressed by the area of 95% confidence ellipses of the scatter of the fingertips at movement end (Fig. 1E). Stimulation of hV6A (or V1/V2) did not appear to influence this measure (Fig. S2A), in line with previous works targeting similar brain regions (Vesia et al. 2010) (Marigold et al. 2019). Effects on precision of depth and direction are reported in the Supplementary material.

Reach end-point accuracy: direction error

The analysis of constant error pattern of reaching end-points revealed a weak main effect of Stimulation Condition ($F_{2,28} = 4.4$, $p = 0.02$, partial $\eta^2 = 0.24$; Fig. 2A and Fig. S3A). This effect appeared driven by a rather small (< 1 mm) but significant increase in direction errors following V1/V2 stimulation (mean values ± SE: 5.6 mm ± 0.34) relative to sham (4.9 mm ± 0.37; $p = 0.009$) and by a similar effect, although non-significant, following hV6A stimulation (5.39 mm ± 0.36; $p = 0.06$). The small increase in direction errors was comparable between the two active conditions ($p = 0.36$) and thus it possibly reflected unspecific effects of active TMS.

Direction error was strongly affected by reaching Direction ($F_{2,28} = 14.99$, $p < 0.001$, partial $\eta^2 = 0.52$; Fig. 2B), and in all cases participants touched the screen to the right of the targets (see positive direction errors in Fig. 2B). The highest direction errors were observed during reaches to the left space (8.03 mm ± 0.71), intermediate to the central space (4.94 mm ± 0.26), lowest to the right (2.99 mm ± 0.78; all comparisons, $p < 0.04$). So, the highest direction errors were observed in the hemispace (left) opposite to the arm used (the right one), as one would expect when the arm moves to the opposite hemifield, given the extra cost to be paid by participants to redirect attention across the vertical meridian with respect to when they have to move attention within one visual quadrant (meridian-crossing effect) (Downing and Pinker 1985; Hughes and Zimba 1985, 1987; Rizzolatti et

al. 1987; Tassinari et al. 1987; Gawryszewski et al. 1992; Reuter-Lorenz and Fendrich 1992).

Reach end-point accuracy: depth error

spTMS delivered over hV6A produced significant depth errors (Fig. 2D), in agreement with the strong influence of the depth of reaching movements in monkey V6A (Hadjidimitrakis, Bertozzi, Breveglieri, Bosco, et al. 2014). Specifically, hV6A stimulation applied 200 ms after the Go signal, during the reaction time, affected depth error for reaches to the farthest targets (Fig. 2D and Fig S3B) as shown by the interaction effect of Stimulation Condition by Stimulation Time by Depth ($F_{4,56}$ = 3.00; p = 0.03, partial η^2 = 0.17). Post-hoc analysis showed no influence of TMS in 100-ms trials across the different target positions (all p > 0.12; see Fig. 2C), but a clear influence of TMS for 200-ms trials, particularly for far target positions, where hV6A stimulation caused larger depth errors (5.29 mm ± 1.48) relative to sham (3.74 mm ± 1.68; p = 0.03) and V1/V2 stimulation (3.37 mm ± 1.26; p = 0.01), which in turn did not differ from one another (p = 0.58).

No significant influence of TMS was observed for intermediate (hV6A: 1.56 mm ± 1.07; V1/V2: 1.95 mm ± 1.01; Sham: 2.93 mm ± 0.83; all comparisons p > 0.05) and near target positions (hV6A: 3.83 mm ± 1.05; V1/V2: 3.60 mm ± 0.89; Sham: 4.64 mm ± 0.62; all comparisons p > 0.15).

In sum, V6A stimulation delivered 200 ms after the Go signal caused hypometric misreaches, in particular when targets were located farther than the gaze position. This suggests an inaccurate encoding of the depth of reaching targets. The increase in hypometric misreach of far targets caused by hV6A stimulation was not associated with changes in action timing as no significant change in reaction times or movement times were detected (reaction time: interaction Stimulation Condition by Stimulation Time by Depth $F_{4,56}$ = 1.56; p = 0.20; partial η^2 = 0.10; movement time: interaction Stimulation Condition by Stimulation Time by Depth, $F_{4,56}$ = 1.99; p = 0.11; partial η^2 = 0.12; see Table S1 for mean values).

Constant reach configuration (peripheral reaching)

Reach end-point precision

Stimulation over hV6A did not influence the end-point precision in the Constant reach configuration when considering Direction (main effect of Stimulation Condition or interactions by Stimulation Condition, all $F < 2.9$, all $p > 0.07$, all partial $\eta^2 < 0.17$). When considering Depth, a significant main effect of Stimulation Condition was found ($F_{2,28} = 4.1$, $p = 0.03$, partial $\eta^2 = 0.23$). Post hoc comparisons revealed that precision after hV6A stimulation did not differ from precision after Sham stimulation (Sham = 6.63$cm^2 \pm 0.75$; hV6A = 6.37 $cm^2 \pm 0.75$; $p = 0.30$, see Fig. S2B). Nevertheless, stimulation over V1/V2 led to an increase in precision of reaching compared to Sham (V1/V2 = 5.93 $cm^2 \pm 0.64$, $p = 0.01$, Fig. S2B), but reaching precision was not different compared to hV6A ($p = 0.09$). Other effects on precision are described in the Supplementary material.

Reach end-point accuracy: direction error

We did not find any significant effects of TMS over hV6A on direction errors (main effect of Stimulation Condition or interaction by Stimulation Condition, all $F < 1.36$, all $p > 0.26$, all partial $\eta^2 < 0.08$). However, similarly to the Constant gaze configuration, in the Constant reach configuration, the reach end-point accuracy was deeply influenced by gaze direction ($F_{2,28} = 21.7$, $p < 0.001$, partial $\eta^2 = 0.61$, Fig. 3A), with gradually larger errors when the gaze was directed to the left of the reaching target, i.e., in the opposite hemispace (5.8 mm ± 0.65) in comparison to the center (3.5 mm ± 0.37) and, in turn, to the right (2.48 mm ± 0.49; all comparisons $p < 0.04$).

Reach end-point accuracy: depth error

Despite the effect observed in depth in the peripheral reaching in Constant gaze configuration, hV6A stimulation did not affect depth errors in Constant reach configuration (main effect of Stimulation Condition or interactions by Stimulation Condition, all $F < 2.61$, all $p > 0.09$, all partial $\eta^2 < 0.16$). This demonstrates that the TMS effect directly acted on the accuracy of arm movement while the decoupling of gaze and hand positions *per se* was not enough to observe it: a change in the final

position of arm movement is also required. Indeed, TMS was effective when the hand reached a position that was farther than the gaze in the Constant gaze configuration, but it was not effective when the hand reached a position that was farther than the gaze in the Constant reach configuration. This suggests that V6A encoding of the depth of reaching is not influenced uniquely by the relative position of hand and gaze (effectiveness of TMS in peripheral but not in foveal reaching), but also by the distance of the hand from the body. This is in agreement with the overwhelming presence in the monkey V6A of neurons with mixed retinotopic/spatial reference frames during reaching (Marzocchi et al. 2008; Hadjidimitrakis, Bertozzi, Breveglieri, Fattori, et al. 2014; Bosco et al. 2016; Hadjidimitrakis et al. 2017).

As figure 3B illustrates, depth strongly influenced the depth error ($F_{2,28} = 34.9$, $p < 0.001$, partial $\eta^2 = 0.71$), leading to a change in its sign (from negative to positive) when gaze position was held near the body during a central reaching (-3.03 mm ± 1.67), resulting in significantly different values relative to when the gaze was held in the intermediate (4.56 mm ± 0.95; $p < 0.001$) and far target position (5.11 mm ± 0.77; $p < 0.001$), which in turn did not differ from one another ($p = 0.61$). We also found a significant, although non-relevant, main effect of Stimulation Time ($F_{1,14} = 8.65$, $p = 0.01$, partial $\eta^2 = 0.38$), with more accurate reaches in the 200-ms trials (1.91 mm ± 0.98) relative to the 100-ms trials (2.50 mm ± 1.06).

Foveal reach configuration (foveal reaching)

Reach end-point precision

Similarly to the other configurations, spTMS on hV6A did not influence the end-point precision in the Foveal reach configuration (all $F < 2.29$, all $p > 0.11$, all partial $\eta^2 < 0.14$, Fig. S2C). The effects of depth and direction on end-point precision, irrespectively of the stimulation, are described in the Supplementary material.

Reach end-point accuracy: direction error

TMS did not influence the direction error (all $F < 0.93$, all $p > 0.4$, all partial $\eta^2 < 0.06$). We observed a strong influence of direction of reaching on end-point accuracy ($F_{2,28} = 10.09$, $p < 0.001$, partial $\eta^2 = 0.42$; Fig. 4A): movements directed to the left space (4.6 mm ± 0.40) were less accurate than movements directed towards the center (3.4 mm ± 0.22; $p = 0.04$) and the right space (2.31 mm ± 0.46; $p < 0.001$), which in turn differ from one another ($p = 0.02$).

Reach end-point accuracy: depth error

We observed a weak borderline effect of Stimulation Condition by Stimulation Time ($F_{2,28} = 3.41$, $p = 0.05$, partial $\eta^2 = 0.19$; Fig. 4B and Fig. S3C). This was driven by an increased tendency to perform hypometric misreaches in 100-ms trials following V1/V2 stimulation (2.57 mm ± 0.53) relative to sham (1.78 mm ± 0.70; $p = 0.006$) and, even though not strictly significant, to hV6A stimulations (2.07 mm ± 0.61; $p = 0.07$), which in turn did not differ from one another ($p = 0.24$). No significant effect of stimulation was observed in 200-ms trials (all $p > 0.09$). Depth strongly influenced depth errors, irrespective of the stimulation condition and time ($F_{2,28} = 11.57$, $p < 0.001$, partial $\eta^2 = 0.45$, Fig. 4C), with reaches to the farthest targets showing greater hypometric errors (3.14 mm ± 0.75) than intermediate (2.35 mm ± 0.51, $p = 0.04$) and near targets (1.4 mm ± 0.56, $p < 0.001$), which in turn differ from one another ($p = 0.01$).

Discussion

In this study, we demonstrated that spTMS delivered over hV6A affects reaching movements towards non-foveated targets (peripheral reaching) located far from the participants' body and from the gaze position. Specifically, stimulation of hV6A during motor planning resulted in an unaltered reaching precision but a consistent decrement in endpoint accuracy, with the endpoints shifting in depth towards the gaze (magnetic misreaching in depth). This decrease in accuracy was not accompanied by effects on reaction time nor on movement time, so we can rule out the possibility that a speed/accuracy trade-off occurred in our participants following brain stimulation.

Our stimulation site was located in the medial exposed surface of PPC, anterior to the parieto-occipital sulcus and medial to the intraparietal sulcus (Fig. 1A), a region that, with different nomenclatures, has been the target of different neuroimaging and TMS studies. In 2008, Culham and coworkers defined the cortical region that included the superior end of the parieto-occipital sulcus and the regions immediately anterior (in the precuneus) and posterior (in the cuneus) to the sulcus as the 'SPOC' (Culham et al. 2008). Note that the anterior part of the SPOC (aSPOC), which roughly corresponds to our stimulation site, likely includes the human homolog of area V6Ad (hV6Ad) (Tosoni et al. 2015). According to Pitzalis and colleagues (Pitzalis et al. 2013), posteriorly and laterally to hV6Ad there is the human homolog of area V6Av and, posterior to it, the human homolog of area V6 (Pitzalis et al. 2015), both regions that were not the focus of our magnetic stimulation. Therefore, according to Pitzalis' lab (Pitzalis et al. 2013; Tosoni et al. 2015), and despite the limited spatial resolution of TMS, we infer that the stimulated area in the present experiment is mostly centered over the hV6Ad. Note that the Talairach coordinates of our stimulation site were the same as those used in another TMS study on hV6A (Ciavarro et al. 2013), and were consistent with those used by Vesia et al. (Vesia et al. 2010).

Given the high percentage of neurons modulated during reach planning in monkey V6A (Santandrea et al. 2018)(Fattori et al. 2005; Hadjidimitrakis, Bertozzi, Breveglieri, Bosco, et al. 2014), we applied TMS to the hV6A, during the movement planning period, after the Go signal and before the movement onset. The single-pulse protocol was used to finely discriminate the timing of causal involvement of hV6A in movement planning. Indeed, it enabled us to demonstrate that only stimulations delivered 200 ms (but not 100 ms) after the Go signal turned out to be effective. This timing is well in keeping with the peak activation in PPC areas after visual stimulation in a reaching task (Bernier et al. 2009)(Fattori et al. 2012). Our results suggest that hV6A elaborates information about the reach plan around 200 ms after the Go signal, that is when target location has presumably been already encoded.

The present results are consistent with the lack of effects in participants' reaching precision observed

by Vesia et al (2010) following hV6A stimulation. Both Vesia et al (Vesia et al. 2010) and Ciavarro et al (Ciavarro et al. 2013) found changes in reaching accuracy after hV6A stimulation, similarly to what we found in the present work, but they did not test reaching movements in depth, that instead we did here. Taken together, the magnetic misreaching in depth found in the current study and that in direction found by others (Ciavarro et al. 2013)(Vesia et al. 2010)(Van Donkelaar and Adams 2005) are consistent with the inability of optic ataxia patients to decouple reach from gaze (Carey et al. 1997; Jackson et al. 2005; Granek et al. 2012). All TMS data demonstrate a causal, crucial role of medial PPC in reaching, as suggested by a plethora of previous correlational studies in both monkeys and humans (Astafiev et al. 2003; Connolly et al. 2003; Prado et al. 2005; Fernandez-Ruiz et al. 2007)(Culham et al., 2008; Filimon et al., 2009; Vesia et al., 2013, 2010; Vesia and Crawford, 2012)(Galletti et al. 2003; Cavina-Pratesi, Monaco, et al. 2010; Galletti and Fattori 2018)(Battaglia-Mayer et al. 1998; Pisella et al. 2000; Snyder et al. 2000; Levy et al. 2007; Tosoni et al. 2008)(Hadjidimitrakis et al. 2011, 2015).

Effect of TMS on peripheral and foveal reaching

In our experiment we asked participants to perform foveal or peripheral reaching using a variety of eye-hand configurations. Surprisingly, despite the high incidence of neurons modulated by the preparation of foveal reaching found in monkey V6A (Fattori et al. 2005; Hadjidimitrakis, Bertozzi, Breveglieri, Bosco, et al. 2014), we did not find any effect when TMS was delivered on hV6A during the planning of foveal reaching. On the other hand, we found that TMS over V1/V2 (but not over hV6A) disrupted planning of foveal reaching when stimulation was administered at 100 ms (but not at 200 ms) after the Go signal. These findings suggest that occipital stimulation acts as a masking of visual information when TMS is administered at 100 ms from stimulus onset, as suggested by previous reports (Amassian et al. 1989; de Graaf et al. 2014). Our findings expand this previous work by showing that interference with visual processing could, in turn, impact motor planning. Moreover, our findings provide evidence of a double dissociation between V1/V2 and hV6A stimulation and

show a specific timing of causal involvement of these brain regions in the planning phase of reaching movements, thus ruling out the influence of unspecific effects.

A clear effect of hV6A stimulation on reaching was only observed for peripheral reaching, in agreement with a previous work reporting that medial PPC regions were activated during peripheral, but not during foveal reaching (Prado et al. 2005). The present results also demonstrate that the spTMS over hV6A altered the reach plan only when reaching was directed farther away with respect to the fixation point. In other words, the effect seemed to be influenced not by the peripheral reaching *per* se, but by the location of reaching target with respect to the fixation point. This means that in hV6A the target of reaching is encoded in a retinal frame of reference, in agreement with fMRI results suggesting that medial PPC encodes visual targets in retinal coordinates (Fernandez-Ruiz et al. 2007). However, the present results also show that when the gaze is directed towards the nearest positions and the targets of reaching are located in the central positions (that is, farther than the gaze), the reaching is not affected. In other words, to elicit reaching impairments after virtual lesions of V6A, it is not enough to have the targets of reaching farther than the location of gaze, but they must be also far from the body. This suggests that hV6A encodes the target of reaching in both retinotopic (farther than the gaze) and spatial (far from the body) frames of references. Alternatively, it could be that hV6A is involved in the remapping of visual target information from a retinotopic to a hand-centered reference frame, a process that may occur during the reaction time, as also suggested by a recent paper (Hadjidimitrakis et al. 2020). All these views are well in agreement with the presence in monkey V6A of neurons with visual receptive fields in retinal, spatial, and in mixed retinal-spatial coordinates (Galletti et al. 1993, 1995; Marzocchi et al. 2008; Bosco et al. 2016)(Bosco et al. 2015)(Hadjidimitrakis, Bertozzi, Breveglieri, Fattori et al. 2014)(Hadjidimitrakis et al. 2020).

While the PPC is commonly viewed as a sensorimotor interface that merges sensory information to plan goal-directed movements, its functional role is still under debate, with sensory-based accounts of PPC organization on the one hand (Bisley and Mirpour 2019) and motor-based accounts on the other (Andersen and Cui 2009). Remarkably, the impairment that we observed here after TMS may

support an alternative view (Medendorp and Heed 2019) which essentially regards the PPC, but also V6A, as a state estimator (Fattori et al. 2017)(Bosco et al 2010)(Grafton, 2010; Shadmehr et al., 2010), which evaluates the current state of the world and body that relates to choosing and specifying the most appropriate actions.

Depth versus direction encoding of reach target.

The decreased accuracy of the amplitude of reaching after hV6A magnetic stimulation found in the present study provides a demonstration of the causal involvement of hV6A in the encoding of reaching, in agreement with the stronger effect of depth than direction of reaching observed in single V6A cells (Hadjidimitrakis, Bertozzi, Breveglieri, Bosco, et al. 2014). Another remarkable demonstration of the causal involvement of V6A in the encoding of reaching comes from a previous lesion study in monkeys where V6A was surgically removed (Battaglini et al. 2002)(Galletti et al. 2003). The animals were strongly impaired in reaching and grasping pieces of food, particularly in the farthest positions of the peripersonal space. The involvement of V6A in depth encoding has also been suggested in optic ataxia patients, whose cortical lesions likely involved area V6A (Galletti et al. 2003)(Karnath and Perenin 2005)(Fattori et al. 2017). In these patients, visuomotor deficits stronger in depth than in direction were repeatedly observed, together with specific impairments of arm movements toward targets arranged at different distances from the body (Holmes and Horrax 1919; Baylis and Baylis 2001; Danckert et al. 2009)(Cavina-Pratesi, Ietswaart, et al. 2010).

Comparison with other TMS studies

Two studies (Vesia et al. 2010; Ciavarro et al. 2013) that applied TMS over a cortical region similar to our stimulation site, reported impairments in the accuracy (direction error) of reaches. In the present work, we observed a similar effect (Fig. 2A), but it was not specifically related to the stimulation of

V1/V2 or hV6A. The reasons for this discrepancy between our data and the above-mentioned studies can be manifold. First, there are differences in the task we used. We employed a visually-guided reaching task, providing the participant with visual information about target location during TMS, whereas the other two studies used a memory-guided reaching (Vesia et al. 2010; Ciavarro et al. 2013). The effect observed in Vesia's and Ciavarro's experiments and the lack of this effect when providing visual information (current study) suggest that the involvement of V6A in reach planning is more marked when visual information is not available. The strong activations of many V6A cells during arm reaching in the dark and the inhibition of several of them in the light (Bosco et al. 2010) agree with this view. Another possible factor that can contribute to the observed discrepancy are the different TMS paradigms: while in Vesia's and Ciavarro's studies a repetitive stimulation was administered (Vesia et al. 2010; Ciavarro et al. 2013), here we used a single pulse paradigm. It is possible that the directional impairments observed by Vesia and Ciavarro are caused by the greater interference with hV6A obtained by using trains of TMS pulses instead of a single pulse.

Previous works demonstrated that V6A neurons receive a strong proprioceptive input from the arms (Breveglieri et al. 2002; Gamberini et al. 2011)(Gamberini et al. 2018) and that the proprioceptive input during reaching is stronger in depth dimension compared to direction (Vindras et al. 1998; Van Beers et al. 2004; Apker et al. 2010). This could explain why, in our experimental conditions, the interference with V6A increased depth errors rather than direction errors.

Our study shows that the accuracy of visually-guided reaching movements in depth is disrupted by hV6A stimulation but not by V1/V2 stimulation. Although site-specific, such effect could be not site-limited. Indeed, it is known that TMS affects neural activity not only locally, but also remote interconnected region (Siebner et al. 2009)(Avenanti et al. 2013)(Valchev et al. 2015). Thus, it is possible that TMS-induced excitation due to hV6A targeting might have spread along other nodes of the dorsomedial stream (Galletti and Fattori 2018) and these nodes might have contributed to the observed changes in reaching performance. Future studies could combine TMS perturbation with EEG or fMRI (Bestmann et al. 2008; Zanon et al. 2018) to monitor the extension of the neural network

altered by hV6A stimulation during motor performance.

Area V6A and the online control of reaching

Monkey V6A contains visual cells with a short latency of activation (about 80 ms)(Kutz et al. 2003; Fattori et al. 2012). This visual information is directly transferred from V6A to the premotor cortex (Matelli et al. 1998; Shipp et al. 1998; Galletti et al. 2004), likely to feed motor centers with vision-for-action information (Fattori et al. 2012). The short latency of visual information coming from V6A is compatible with the fast motor response of an automatic system that performs unconscious online corrections of the direction of movement in the case of unexpected target jumps after movement onset (Goodale et al. 1986; Pélisson et al. 1986; Paulignan et al. 1991; Prablanc and Martin 1992). The presence in V6A of many neurons modulated during reaching execution (Fattori et al. 2001, 2005, 2017; Bosco et al. 2010; Hadjidimitrakis, Bertozzi, Breveglieri, Bosco, et al. 2014) as well as by visual stimulation (Breveglieri et al. 2015)(Gamberini et al. 2011; Fattori et al. 2012) suggests that this area could participate in the online monitoring of arm movement during reaching and could be involved in the correction of ongoing arm movement in case of perturbation of reach target location (Galletti et al. 2003; Rizzolatti and Matelli 2003; Galletti and Fattori 2018). However, despite the intriguing above-reported suggestion, no study to date has demonstrated the presence of V6A neurons modulated by changes of reaching trajectory evoked by sudden target displacements. Conversely, such a type of neurons have been reported in the lateral PPC (specifically, in the lateral part of area PE) (Archambault et al. 2009, 2015; Battaglia-Mayer et al. 2013), and in agreement with these data, TMS on the lateral PPC disrupted the path corrections that normally occur in response to target jumps (Desmurget et al. 1999)(Reichenbach et al. 2014)(Reichenbach et al. 2011). In other words, previous data suggest that the lateral PPC is involved in the online correction of arm movements, whereas the present findings indicate that the medial PPC is involved in the planning of movement and/or in remapping target information between different reference frames. Whether V6A is also causally involved in the online control of reaching movement is a question that remains open, because to check

this point one should apply TMS during the movement time instead of reaction time as in the present case. Further experiments with this goal are needed to clarify this point.

Acknowledgments/funding

This work was supported by grants from the Fondazione Cassa di Risparmio in Bologna (Grant CARISBO internazionalizzazione 2019), and the Ministero dell'Università e della Ricerca (MIUR, PRIN2017KZNZLN) awarded to PF. AA is supported by grants from the Fondazione del Monte di Bologna e Ravenna (339bis/2017), the Bial Foundation (347/18) and the Ministero dell'Università e della Ricerca (2017N7WCLP). SB is supported by grants from the Ministero della Salute, Italy (GR-2018-12365733).

Address of the corresponding author: rossella.breveglieri@unibo.it.

References

Amassian VE, Cracco RQ, Maccabee PJ, Cracco JB, Rudell A, Eberle L. 1989. Suppression of visual perception by magnetic coil stimulation of human occipital cortex. Electroencephalogr Clin Neurophysiol Evoked Potentials. 74:458–462.

Amemiya T, Beck B, Walsh V, Gomi H, Haggard P. 2017. Visual area V5/hMT+ contributes to perception of tactile motion direction: A TMS study. Sci Rep. 7:40937.

Andersen RA, Snyder LH, Bradley DC, Xing J. 1997. Multimodal representation of space in the posterior parietal cortex and its use in planning movements. Annu Rev Neurosci. 20:303–330.

Andersen RA, Cui H. 2009. Intention, action planning, and decision making in parietal-frontal circuits. Neuron. 63:568–583.

Apker GA, Darling TK, Buneo CA. 2010. Interacting noise sources shape patterns of arm

movement variability in three-dimensional space. J Neurophysiol. 104:2654–2666.

Archambault PS, Caminiti R, Battaglia-Mayer A. 2009. Cortical mechanisms for online control of hand movement trajectory: The role of the posterior parietal cortex. Cereb Cortex. 19:2848–2864.

Archambault PS, Ferrari-Toniolo S, Caminiti R, Battaglia-Mayer A. 2015. Visually-guided correction of hand reaching movements: The neurophysiological bases in the cerebral cortex. Vision Res. 110:244–256.

Astafiev S V., Shulman GL, Stanley CM, Snyder AZ, Van Essen DC, Corbetta M. 2003. Functional organization of human intraparietal and frontal cortex for attending, looking, and pointing. J Neurosci. 23:4689–4699.

Avenanti A, Paracampo R, Annella L, Tidoni E, Aglioti SM. 2018. Boosting and decreasing action prediction abilities through excitatory and inhibitory tDCS of inferior frontal cortex. Cereb Cortex 28(4):1282-1296.

Avenanti A, Annella L, Candidi M, Urgesi C, Aglioti SM. 2013. Compensatory plasticity in the action observation network: Virtual lesions of STS enhance anticipatory simulation of seen actions. Cereb Cortex. 23:570–580.

Battaglia-Mayer A, Ferraina S, Marconi B, Bullis JB, Lacquaniti F, Burnod Y, Baraduc P, Caminiti R. 1998. Early motor influences on visuomotor transformations for reaching: A positive image of optic ataxia. Exp Brain Res. 123:172–189.

Battaglia-Mayer A, Ferrari-Toniolo S, Visco-Comandini F, Archambault PS, Saberi-Moghadam S, Caminiti R. 2013. Impairment of online control of hand and eye movements in a monkey model of optic ataxia. Cereb Cortex. 23:2644–2656.

Battaglini P, Muzur A, Galletti C, Skrap M, Brovelli A, Fattori P. 2002. Effects of lesions to area V6A in monkeys. Exp Brain Res. 144:419–422.

Baylis GC, Baylis LL. 2001. Visually misguided reaching in Balint's syndrome. Neuropsychologia. 39:865–875.

Bernier PM, Burle B, Hasbroucq T, Blouin J. 2009. Spatio-temporal dynamics of reach-related neural activity for visual and somatosensory targets. Neuroimage. 47:1767–1777.

Bestmann S, Swayne O, Blankenburg F, Ruff CC, Haggard P, Weiskopf N, Josephs O, Driver J, Rothwell JC, Ward NS. 2008. Dorsal premotor cortex exerts state-dependent causal influences on activity in contralateral primary motor and dorsal premotor cortex. Cereb Cortex. 18:1281–1291.

Bisley JW, Mirpour K. 2019. The neural instantiation of a priority map. Curr Opin Psychol. 29:108–112

Blangero A, Menz MM, McNamara A, Binkofski F. 2009. Parietal modules for reaching. Neuropsychologia. 47:1500–1507.

Bosco A, Breveglieri R, Chinellato E, Galletti C, Fattori P. 2010. Reaching activity in the medial posterior parietal cortex of monkeys is modulated by visual feedback. J Neurosci. 30:14773–14785.

Bosco A, Breveglieri R, Hadjidimitrakis K, Galletti C, Fattori P. 2016. Reference frames for reaching when decoupling eye and target position in depth and direction. Sci Rep. 6:21646.

Bosco A, Breveglieri R, Reser D, Galletti C, Fattori P. 2015. Multiple representation of reaching space in the medial posterior parietal area V6A. Cereb Cortex. 25:1654–1667.

Bosco A, Piserchia V, Fattori P. 2017. Multiple Coordinate Systems and Motor Strategies for Reaching Movements When Eye and Hand Are Dissociated in Depth and Direction. Front Hum Neurosci. 11:323.

Brainard DH. 1997. The Psychophysics Toolbox. Spat Vis 10, 433–436.

Breveglieri R, Galletti C, Bosco A, Gamberini M, Fattori P. 2015. Object affordance modulates visual responses in the macaque medial posterior parietal cortex. J Cogn Neurosci. 27:1447–1455.

Breveglieri R, Kutz DF, Fattori P, Gamberini M, Galletti C. 2002. Somatosensory cells in the parieto-occipital area V6A of the macaque. Neuroreport. 13:2113–2116.

Briggs GG, Nebes RD. 1975. Patterns of Hand Preference in a Student Population. Cortex 11:230-8.

Buelte D, Meister IG, Staedtgen M, Dambeck N, Sparing R, Grefkes C, Boroojerdi B. 2008. The role of the anterior intraparietal sulcus in crossmodal processing of object features in humans: an rTMS study. Brain Res. 1217:110–118.

Carducci F, Brusco R. 2012. Accuracy of an individualized MR-based head model for navigated brain stimulation. Psychiatry Res - Neuroimaging 203(1):105-8.

Carey DP, Coleman RJ, Sala S Della. 1997. Magnetic misreaching. Cortex. 33:639–652.

Cavina-Pratesi C, Ietswaart M, Humphreys GW, Lestou V, Milner AD. 2010. Impaired grasping in a patient with optic ataxia: Primary visuomotor deficit or secondary consequence of misreaching? Neuropsychologia. 48:226–234.

Cavina-Pratesi C, Monaco S, Fattori P, Galletti C, McAdam TD, Quinlan DJ, Goodale MA, Culham JC. 2010. Functional magnetic resonance imaging reveals the neural substrates of arm transport and grip formation in reach-to-grasp actions in humans. J Neurosci. 30:10306–10323.

Chiappini E, Silvanto J, Hibbard PB, Avenanti A, Romei V. 2018. Strengthening functionally specific neural pathways with transcranial brain stimulation. Curr Biol. 28:R735–R736.

Ciavarro M, Ambrosini E, Tosoni A, Committeri G, Fattori P, Galletti C. 2013. rTMS of Medial Parieto-occipital Cortex Interferes with Attentional Reorienting during Attention and Reaching Tasks. J Cogn Neurosci. 1–10.

Colby CL, Goldberg ME. 1999. Space and attention in the parietal cortex. Annu Rev Neurosci. 22:319–349.

Connolly JD, Andersen RA, Goodale MA. 2003. FMRI evidence for a “parietal reach region” in the human brain. Exp Brain Res. 153:140–145.

Culham JC, Cavina-Pratesi C, Singhal A. 2006. The role of parietal cortex in visuomotor control: What have we learned from neuroimaging? Neuropsychologia. 44:2668–2684.

Culham JC, Gallivan J, Cavina-Pratesi C, Quinlan DJ. 2008. fMRI investigations of reaching and

ego space in human superior parieto-occipital cortex. In: Klatzky R,, McWhinney B,, Behrmann M, editors. Embodiment, ego-space and action. p. 247–274.

Culham JC, Valyear KF. 2006. Human parietal cortex in action. Curr Opin Neurobiol. 16:205–212.

Dambeck N, Sparing R, Meister IG, Wienemann M, Weidemann J, Topper R, Boroojerdi B. 2006. Interhemispheric imbalance during visuospatial attention investigated by unilateral and bilateral TMS over human parietal cortices. Brain Res. 1072:194–199.

Danckert J, Goldberg L, Broderick C. 2009. Damage to superior parietal cortex impairs pointing in the sagittal plane. Exp Brain Res. 195:183–191.

de Graaf TA, Koivisto M, Jacobs C, Sack AT. 2014. The chronometry of visual perception: Review of occipital TMS masking studies. Neurosci Biobehav Rev. 45:295–304.

Delle Monache S, Lacquaniti F, Bosco G. 2017. Differential contributions to the interception of occluded ballistic trajectories by the temporoparietal junction, area hMT/V5+, and the intraparietal cortex. J Neurophysiol. 118:1809–1823.

Desmurget M, Epstein CM, Turner RS, Prablanc C, Alexander GE, Grafton ST. 1999. Role of the posterior parietal cortex in updating reaching movements to a visual target. Nat Neurosci. 2:563–567.

Dessing JC, Vesia M, Douglas Crawford J. 2013. The role of areas MT+/V5 and SPOC in spatial and temporal control of manual interception: An rTMS study. Front Behav Neurosci. 7–15.

Downing CJ, Pinker S. 1985. The spatial structure of visual attention. Atten Perform XI.

Fattori P, Breveglieri R, Bosco A, Gamberini M, Galletti C. 2017. Vision for Prehension in the Medial Parietal Cortex. Cereb Cortex. 27:1149–1163.

Fattori P, Breveglieri R, Raos V, Bosco A, Galletti C. 2012. Vision for action in the macaque medial posterior parietal cortex. J Neurosci. 32:3221–3234.

Fattori P, Gamberini M, Kutz DF, Galletti C. 2001. “Arm-reaching” neurons in the parietal area V6A of the macaque monkey. Eur J Neurosci. 13:2309–2313.

Fattori P, Kutz DF, Breveglieri R, Marzocchi N, Galletti C. 2005. Spatial tuning of reaching activity

in the medial parieto-occipital cortex (area V6A) of macaque monkey. Eur J Neurosci. 22:956–972.

Faul F, Erdfelder E, Lang A, Buchner A. 2007. G*Power 3: A flexible statistical power analysis program for the social, behavioral, and biomedical sciences. Behav Res Methods. 39:175–191.

Fernandez-Ruiz J, Goltz HC, DeSouza JFX, Vilis T, Crawford JD. 2007. Human parietal "reach region" primarily encodes intrinsic visual direction, not extrinsic movement direction, in a visual-motor dissociation task. Cereb Cortex. 17:2283–2292.

Filimon F. 2010. Human cortical control of hand movements: Parietofrontal networks for reaching, grasping, and pointing. Neuroscientist. 16:388–407.

Filimon F, Nelson JD, Huang RS, Sereno MI. 2009. Multiple parietal reach regions in humans: Cortical representations for visual and proprioceptive feedback during on-line reaching. J Neurosci. 29:2961–2971.

Fisher DF, Monty RA, Senders JW. 2017. Eye Movements: Cognition and Perception. Psychology. ed.

Galletti C, Battaglini PP, Fattori P. 1993. Parietal neurons encoding spatial locations in craniotopic coordinates. Exp Brain Res. 96:221–229.

Galletti C, Battaglini PP, Fattori P. 1995. Eye Position Influence on the Parieto-occipital Area PO (V6) of the Macaque Monkey. Eur J Neurosci. 7:2486–2501.

Galletti C, Fattori P. 2018. The dorsal visual stream revisited: Stable circuits or dynamic pathways? Cortex. S0010-9452(17)30015-1.

Galletti C, Fattori P, Gamberini M, Kutz D. 2004. The most direct visual pathway to the frontal cortex. Cortex. 40:216–217.

Galletti C, Fattori P, Kutz DF, Gamberini M. 1999. Brain location and visual topography of cortical area V6A in the macaque monkey. Eur J Neurosci. 11:575–582.

Galletti C, Kutz DF, Gamberini M, Breveglieri R, Fattori P. 2003. Role of the medial parieto-occipital cortex in the control of reaching and grasping movements. Experimental Brain

Research. p. 158–170.

Gallivan JP, Cavina-Pratesi C, Culham JC. 2009. Is that within reach? fMRI reveals that the human superior parieto-occipital cortex encodes objects reachable by the hand. J Neurosci. 29:4381–4391.

Gallivan JP, McLean A, Culham JC. 2011. Neuroimaging reveals enhanced activation in a reach-selective brain area for objects located within participants' typical hand workspaces. Neuropsychologia. 49:3710–3721.

Gamberini M, Galletti C, Bosco A, Breveglieri R, Fattori P. 2011. Is the medial posterior parietal area V6A a single functional area? J Neurosci. 31:5145–5157.

Gamberini M, Dal Bò G, Breveglieri R, Briganti S, Passarelli L, Fattori P, Galletti C. 2018. Sensory properties of the caudal aspect of the macaque's superior parietal lobule. Brain Struct Funct. 223:1–17.

Gawryszewski L, Faria RB, Thomaz TG, Pinheiro WM, Rizzolatti G, Umilta C. 1992. Reorienting Visual Spatial Attention: Is It Based on Cartesian Coordinates? In: The Visual System from Genesis to Maturity.

Goodale MA, Milner AD. 1992. Separate visual pathways for perception and action. Trends Neurosci. 15:20–25.

Goodale MA, Pelisson D, Prablanc C. 1986. Large adjustments in visually guided reaching do not depend on vision of the hand or perception of target displacement. Nature. 320:748–750.

Granek JA, Pisella L, Blangero A, Rossetti Y, Sergio LE. 2012. The Role of the Caudal Superior Parietal Lobule in Updating Hand Location in Peripheral Vision: Further Evidence from Optic Ataxia. PLoS One. 7:e46619.

Grafton ST. 2010. The cognitive neuroscience of prehension: Recent developments. Exp Brain Res 204(4):475-91.

Hadjidimitrakis K, Breveglieri R, Placenti G, Bosco A, Sabatini SPSP, Fattori P. 2011. Fix your eyes in the space you could reach: Neurons in the macaque medial parietal cortex prefer gaze

positions in peripersonal space. PLoS One. 6:e23335.

Hadjidimitrakis K, Dal Bo' G, Breveglieri R, Galletti C, Fattori P. 2015. Overlapping representations for reach depth and direction in caudal superior parietal lobule of macaques. J Neurophysiol. 114:2340–2352.

Hadjidimitrakis K, Bertozzi F, Breveglieri R, Bosco A, Galletti C, Fattori P. 2014. Common neural substrate for processing depth and direction signals for reaching in the monkey medial posterior parietal cortex. Cereb Cortex. 24:1645–1657.

Hadjidimitrakis K, Bertozzi F, Breveglieri R, Fattori P, Galletti C. 2014. Body-Centered, Mixed, but not Hand-Centered Coding of Visual Targets in the Medial Posterior Parietal Cortex During Reaches in 3D Space. Cereb Cortex. 24:3209–3220.

Hadjidimitrakis K, Bertozzi F, Breveglieri R, Galletti C, Fattori P. 2017. Temporal stability of reference frames in monkey area V6A during a reaching task in 3D space. Brain Struct Funct. 222:1959–1970.

Hadjidimitrakis K, Ghodrati M, Breveglieri R, Rosa MGP, Fattori P. 2020. Neural coding of action in three dimensions: Task- and time-invariant reference frames for visuospatial and motor-related activity in parietal area V6A. J Comp Neurol. doi: 10.10.

Holmes G, Horrax G. 1919. Disturbances of spatial orientation and visual attention, with loss of stereoscopic vision. Arch Neurol Psychiatry 1:385-407.

Hughes HC, Zimba LD. 1985. Spatial Maps of Directed Visual Attention. J Exp Psychol Hum Percept Perform. 11:409–430.

Hughes HC, Zimba LD. 1987. Natural boundaries for the spatial spread of directed visual attention. Neuropsychologia. 25:5–18.

Jackson SR, Newport R, Mort D, Husain M. 2005. Where the eye looks, the hand follows: Limb-dependent magnetic misreaching in optic ataxia. Curr Biol. 15:42–46.

Jeannerod M, Arbib MA, Rizzolatti G, Sakata H. 1995. Grasping objects: the cortical mechanisms of visuomotor transformation. Trends Neurosci. 18:314–320.

Jacquet PO, Avenanti A. 2015. Perturbing the action observation network during perception and categorization of actions' goals and grips: State-dependency and virtual lesion TMS effects. Cereb Cortex. 25:598–608.

Kamitani Y, Shimojo S. 1999. Manifestation of scotomas created by transcranial magnetic stimulation of human visual cortex. Nat Neurosci. 2:767–771.

Karnath HO, Perenin MT. 2005. Cortical control of visually guided reaching: Evidence from patients with optic ataxia. Cereb Cortex. 15:1561–1569.

Kutz DF, Fattori P, Gamberini M, Breveglieri R, Galletti C. 2003. Early- and late-responding cells to saccadic eye movements in the cortical area V6A of macaque monkey. Exp Brain Res. 149:83–95.

Levkovitz Y, Marx J, Grisaru N, Segal M. 1999. Long-term effects of transcranial magnetic stimulation on hippocampal reactivity to afferent stimulation. J Neurosci. 19:3198–3203.

Levy I, Schluppeck D, Heeger DJ, Glimcher PW. 2007. Specificity of human cortical areas for reaches and saccades. J Neurosci. 27:4687–4696.

Lewald J, Foltys H, Töpper R. 2002. Role of the posterior parietal cortex in spatial hearing. J Neurosci. 22:RC207.

Lisanby SH, Gutman D, Luber B, Schroeder C, Sackeim HA. 2001. Sham TMS: Intracerebral measurement of the induced electrical field and the induction of motor-evoked potentials. Biol Psychiatry. 49:460–463.

Lockwood PL, Iannetti GD, Haggard P. 2013. Transcranial magnetic stimulation over human secondary somatosensory cortex disrupts perception of pain intensity. Cortex. 49:2201–2209.

Marigold DS, Lajoie K, Heed T. 2019. No effect of triple-pulse TMS medial to intraparietal sulcus on online correction for target perturbations during goal-directed hand and foot reaches. PLoS One. 14:e0223986.

Marzocchi N, Breveglieri R, Galletti C, Fattori P. 2008. Reaching activity in parietal area V6A of macaque: eye influence on arm activity or retinocentric coding of reaching movements? Eur J

Neurosci. 27:775–789.

Matelli M, Govoni P, Galletti C, Kutz DF, Luppino G. 1998. Superior area 6 afferents from the superior parietal lobule in the macaque monkey. J Comp Neurol. 402:327–352.

Medendorp WP, Heed T. 2019. State estimation in posterior parietal cortex: Distinct poles of environmental and bodily states. Prog Neurobiol. 183:101691

Monaco S, Chen Y, Medendorp WP, Crawford JD, Fiehler K, Henriques DYP. 2014. Functional magnetic resonance imaging adaptation reveals the cortical networks for processing grasp-relevant object properties. Cereb Cortex. 24:1540–1554.

Paracampo R, Pirruccio M, Costa M, Borgomaneri S, Avenanti A. 2018. Visual, sensorimotor and cognitive routes to understanding others' enjoyment: An individual differences rTMS approach to empathic accuracy. Neuropsychologia. 116:86–98.

Pascual-Leone A, Bartres-Faz D, Keenan JP. 1999. Transcranial magnetic stimulation: Studying the brain-behaviour relationship by induction of "virtual lesions." Philos Trans R Soc B Biol Sci. 354:1229–1238.

Pascual-leone A, Valls-solé J, Wassermann EM, Hallett M. 1994. Responses to rapid-rate transcranial magnetic stimulation of the human motor cortex. Brain. 117:847–858.

Paulignan Y, MacKenzie C, Marteniuk R, Jeannerod M. 1991. Selective perturbation of visual input during prehension movements - 1. The effects of changing object position. Exp Brain Res. 83:502–512.

Pélisson D, Prablanc C, Goodale MA, Jeannerod M. 1986. Visual control of reaching movements without vision of the limb - II. Evidence of fast unconscious processes correcting the trajectory of the hand to the final position of a double-step stimulus. Exp Brain Res. 62:303–311.

Perenin M-T, Vighetto A. 1983. Optic ataxia: A specific disorder in visuomotor coordination. In: Spatially oriented behavior. p. 305–326.

Perenin MT, Vighetto A. 1988. Optic ataxia: A specific disruption in visuomotor mechanisms: I. Different aspects of the deficit in reaching for objects. Brain. 111:643–674.

Pisella L, Gréa H, Tilikete C, Vighetto A, Desmurget M, Rode G, Boisson D, Rossetti Y. 2000. An "automatic pilot" for the hand in human posterior parietal cortex: Toward reinterpreting optic ataxia. Nat Neurosci. 3:729–736.

Pitzalis S, Fattori P, Galletti C. 2015. The human cortical areas V6 and V6A. Vis Neurosci. 32, e00X,:E007.

Pitzalis S, Sereno MI, Committeri G, Fattori P, Galati G, Tosoni A, Galletti C. 2013. The human homologue of macaque area V6A. Neuroimage. 82:517–530.

Prablanc C, Martin O. 1992. Automatic control during hand reaching at undetected two-dimensional target displacements. J Neurophysiol. 67:455–469.

Prado J, Clavagnier S, Otzenberger H, Scheiber C, Kennedy H, Perenin MT. 2005. Two cortical systems for reaching in central and peripheral vision. Neuron. 48:849–858.

Prime SL, Vesia M, Crawford JD. 2008. Transcranial magnetic stimulation over posterior parietal cortex disrupts transsaccadic memory of multiple objects. J Neurosci. 28:6938–6949.

Reichenbach A, Bresciani JP, Peer A, Bülthoff HH, Thielscher A. 2011. Contributions of the PPC to online control of visually guided reaching movements assessed with fMRI-Guided TMS. Cereb Cortex. 21:1602–1612.

Reichenbach A, Thielscher A, Peer A, Bülthoff HH, Bresciani JP. 2014. A key region in the human parietal cortex for processing proprioceptive hand feedback during reaching movements. Neuroimage. 84:615–625.

Reuter-Lorenz PA, Fendrich R. 1992. Oculomotor readiness and covert orienting: Differences between central and peripheral precues. Percept Psychophys. 52:336–344.

Rizzolatti G, Matelli M. 2003. Two different streams form the dorsal visual system: Anatomy and functions. In: Experimental Brain Research. p. 146–157.

Rizzolatti G, Riggio L, Dascola I, Umiltá C. 1987. Reorienting attention across the horizontal and vertical meridians: Evidence in favor of a premotor theory of attention. Neuropsychologia. 25:31–40.

Romei V, Chiappini E, Hibbard PB, Avenanti A. 2016. Empowering Reentrant Projections from V5 to V1 Boosts Sensitivity to Motion. Curr Biol 26:2155-60.

Rossetti Y, Revol P, McIntosh R, Pisella L, Rode G, Danckert J, Tilikete C, Dijkerman HC, Boisson D, Vighetto A, Michel F, Milner AD. 2005. Visually guided reaching: Bilateral posterior parietal lesions cause a switch from fast visuomotor to slow cognitive control. Neuropsychologia. 43:162–177.

Rossi S, Hallett M, Rossini PM, Pascual-Leone A, Safety of TMS Consensus Group. 2009. Safety, ethical considerations, and application guidelines for the use of transcranial magnetic stimulation in clinical practice and research. Clin Neurophysiol. 120:2008–2039.

Rossit S, McAdam T, Mclean DA, Goodale MA, Culham JC. 2013. FMRI reveals a lower visual field preference for hand actions in human superior parieto-occipital cortex (SPOC) and precuneus. Cortex. 49:2525–2541.

Sandrini M, Umiltà C, Rusconi E. 2011. The use of transcranial magnetic stimulation in cognitive neuroscience: A new synthesis of methodological issues. Neurosci Biobehav Rev. 35:516–536.

Santandrea E, Breveglieri R, Bosco A, Galletti C, Fattori P. 2018. Preparatory activity for purposeful arm movements in the dorsomedial parietal area V6A: Beyond the online guidance of movement. Sci Rep. 8:6926.

Shadmehr R, Smith MA, Krakauer JW. 2010. Error Correction, Sensory Prediction, and Adaptation in Motor Control. Annu Rev Neurosci. 20:726–730.

Shipp S, Blanton M, Zeki S. 1998. A visuo-somatomotor pathway through superior parietal cortex in the macaque monkey: Cortical connections of areas V6 and V6A. Eur J Neurosci. 10:3171–3193.

Siebner HR, Hartwigsen G, Kassuba T, Rothwell JC. 2009. How does transcranial magnetic stimulation modify neuronal activity in the brain? Implications for studies of cognition. Cortex. 45:1035–1042.

Siebner HR, Rothwell J. 2003. Transcranial magnetic stimulation: New insights into

representational cortical plasticity. Exp Brain Res. 148:1–16.

Smyrnis N, Theleritis C, Evdokimidis I, Müri RM, Karandreas N. 2003. Single-pulse transcranial magnetic stimulation of parietal and prefrontal areas in a memory delay arm pointing task. J Neurophysiol. 89:3344–3350.

Snyder LH, Batista AP, Andersen RA. 2000. Intention-related activity in the posterior parietal cortex: A review. Vision Res. 40:1433–1441.

Talairach J, Tournoux P. 1988. Co-planar stereotaxic atlas of the human brain: 3-dimensional proportional system: an approach to cerebral imaging. Stuttgart, NY.

Tassinari G, Aglioti S, Chelazzi L, Marzi CA, Berlucchi G. 1987. Distribution in the visual field of the costs of voluntarily allocated attention and of the inhibitory after-effects of covert orienting. Neuropsychologia. 25:55–71.

Tosoni A, Galati G, Romani GL, Corbetta M. 2008. Sensory-motor mechanisms in human parietal cortex underlie arbitrary visual decisions. Nat Neurosci. 11:1446–1453.

Tosoni A, Pitzalis S, Committeri G, Fattori P, Galletti C, Galati G. 2015. Resting-state connectivity and functional specialization in human medial parieto-occipital cortex. Brain Struct Funct. 220:3307–3321.

Valchev N, Curčić-Blake B, Renken RJ, Avenanti A, Keysers C, Gazzola V, Maurits NM. 2015. cTBS delivered to the left somatosensory cortex changes its functional connectivity during rest. Neuroimage. 114:386–397.

Valchev N, Tidoni E, Hamilton AF d. C, Gazzola V, Avenanti A. 2017. Primary somatosensory cortex necessary for the perception of weight from other people's action: A continuous theta-burst TMS experiment. Neuroimage 152:195-206.

Vallar G, Branch Coslett H. 2018. Handbook of clinical neurology. The parietal lobe.

Van Beers RJ, Haggard P, Wolpert DM. 2004. The Role of Execution Noise in Movement Variability. J Neurophysiol. 91:1050–1063.

Van Donkelaar P, Adams J. 2005. Gaze-dependent deviation in pointing induced by transcranial

magnetic stimulation over the human posterior parietal cortex. J Mot Behav. 37:157–163.

Vesia M, Barnett-Cowan M, Elahi B, Jegatheeswaran G, Isayama R, Neva JL, Davare M, Staines WR, Culham JC, Chen R. 2017. Human dorsomedial parieto-motor circuit specifies grasp during the planning of goal-directed hand actions. Cortex. 92:175–186.

Vesia M, Bolton DA, Mochizuki G, Staines WR. 2013. Human parietal and primary motor cortical interactions are selectively modulated during the transport and grip formation of goal-directed hand actions. Neuropsychologia. 51:410–417.

Vesia M, Crawford JD. 2012. Specialization of reach function in human posterior parietal cortex. Exp Brain Res. 221:1–18.

Vesia M, Monteon JA, Sergio LE, Crawford JD. 2006. Hemispheric asymmetry in memory-guided pointing during single-pulse transcranial magnetic stimulation of human parietal cortex. J Neurophysiol. 96:3016–3027.

Vesia M, Prime SL, Yan X, Sergio LE, Crawford JD. 2010. Specificity of human parietal saccade and reach regions during transcranial magnetic stimulation. J Neurosci. 30:13053–13065.

Vesia M, Yan X, Henriques DY, Sergio LE, Crawford JD. 2008. Transcranial magnetic stimulation over human dorsal-lateral posterior parietal cortex disrupts integration of hand position signals into the reach plan. J Neurophysiol. 100:2005–2014.

Vindras P, Desmurget M, Prablanc C, Viviani P. 1998. Pointing errors reflect biases in the perception of the initial hand position. J Neurophysiol. 79:3290–3294.

Wang H, Wang X, Scheich H. 1996. LTD and LTP induced by transcranial magnetic stimulation in auditory cortex. Neuroreport. 7:521–525.

Zanon M, Borgomaneri S, Avenanti A. 2018. Action-related dynamic changes in inferior frontal cortex effective connectivity: A TMS/EEG coregistration study. Cortex. 108:193–209.

Captions to figures

Figure 1)

Experimental setup A) Targeted hV6A site (indicated with white crosses) displayed in a Transverse (top left), Sagittal (bottom) and Coronal (top right) template brain section in one exemplary subject. POs= parieto-occipital sulcus. B) Top (left) and lateral (right) view of the target arrangement in the experimental task. The participants performed reaching movements with their right hand towards one of the nine targets (gray dots) located at different depths (far, intermediate and near) and in different directions (left, center and right). Reaching movements were performed in a darkened room from the initial hand position located next to the body (Home button), indicated by a square. C) Top view of the three task configurations. Top panel, Constant gaze configuration: reaching movements were performed towards one of the nine targets (hands). The spatial position of the target changed trial to trial, but the gaze was kept constant at the central position. Central panel, Constant reach configuration: reaching movements were always performed towards the target located in the central position. During the execution of the task, participants had to fixate one of the nine different positions (eyes). Bottom panel, Foveal reach configuration: reaching movements were performed towards one of the nine targets. During the task, the participant fixated and reached the same target (eye and hand on the panel). D) Time sequence of visually-guided reaching (only Constant gaze configuration is shown for conciseness). The small eye depicted in the figure represents the fixation point; the filled black dot represents the reaching target. The fixation point (a green point on the touchscreen) stayed on for 1.3 or 1.5 s and then the reaching target (a red point on the touchscreen) was turned on in one of the locations. Immediately, the participant had to reach with her/his right hand the visible position of the target while maintaining fixation on the fixation target (immediate reaching). During the reaction time, spTMS was delivered after 100 ms (100ms-trial) or 200 ms (200ms-trial). The fixation and the reaching targets were visible until the participant completed the movement. E) Sketch of the measurements of the precision and the accuracy of the reaching movements. An exemplary 95% confidence ellipse is shown, as well as the indication of depth and direction errors. ‘Target’ represents the reaching target.

Figure 2)

Accuracy in the Constant gaze configuration. A) Distribution of direction errors in TMS delivered during Sham stimulation (SHAM, white), V1/V2 stimulation (V1/V2, dark gray) and hV6A stimulation (hV6A, black). A main effect of the Stimulation condition was evident, due to a decrease in accuracy after V1/V2 stimulation. B) Distribution of direction errors in the different directions of reaching. LEFT= left targets, INT=intermediate targets, RIGHT=right targets. Accuracy was influenced by the direction of reaching. C) Distribution of depth errors in the different stimulation conditions at different depths of reaching during 100-ms trials. No effect of TMS is shown. D) Distribution of depth errors in the different stimulation conditions at different depths of reaching during 200-ms trials. After spTMS over hV6A after 200 ms from the Go signal, reaching movements towards far targets were performed less accurately. FAR=reaching targets far from the body, INT=intermediate reaching targets, NEAR=reaching target near to the body. Asterisks indicate significant posthoc comparisons ($p<0.05$).

Figure 3)

Accuracy in the Constant reach configuration. A) Influence of the direction of the gaze position on direction errors, shown by the distribution of direction errors for reaching movements executed when the gaze was at different directions. Accuracy varied as a function of gaze position. B) Effect of depth of the gaze position on the depth errors, as shown by the distribution of depth errors for reaching movements executed when the gaze was at different depths (FAR=gaze positions far from the body, INT=intermediate gaze positions, NEAR=gaze positions near to the body). The depth of the gaze position influenced the reach accuracy. Other conventions as in figure 2.

Figure 4)

Accuracy in the Foveal reach configuration. A) Effect of the direction of reaching on the direction errors, as shown by the distribution of direction errors for reaching movements executed toward

targets located at different directions. The direction of foveal reaching influenced the reaching accuracy. B) Distribution of depth errors in 100-ms trials and in 200-ms trials in the different stimulation conditions. Stimulation of V1/V2 at 100 ms decreased the reaching accuracy. C) Effect of depth of reaching on the depth errors, as shown by the distribution of depth errors for reaching at different depths. Accuracy of reaching at different depths differed. Other conventions as in figure 2.

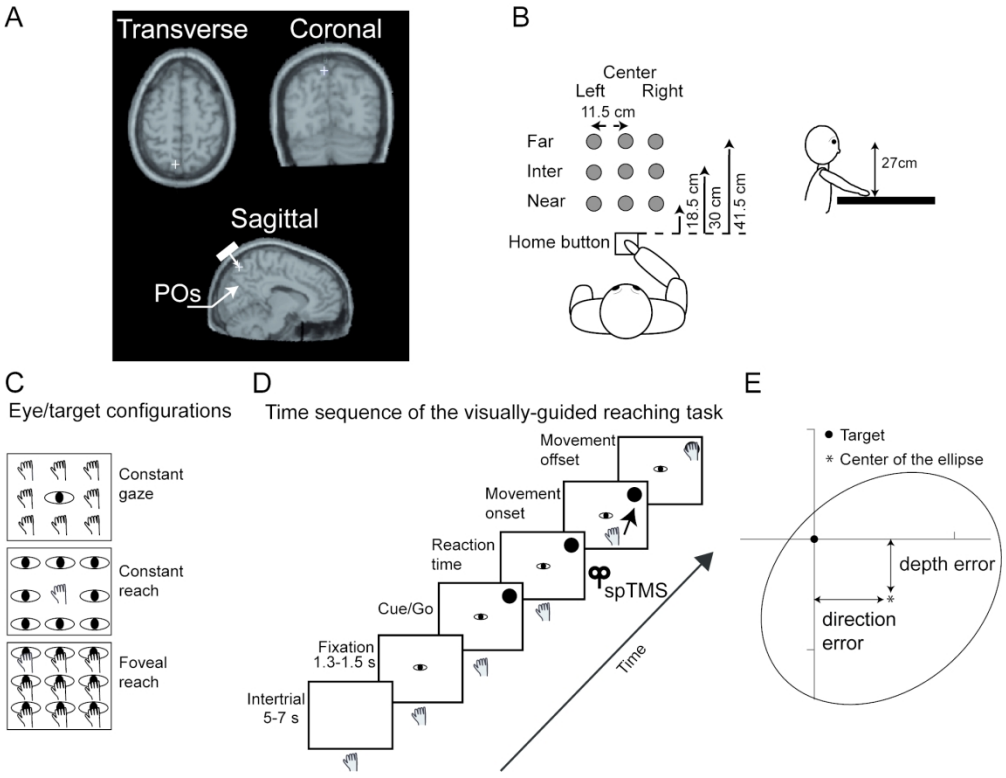

Figure 1

Experimental setup A) Targeted hV6A site (indicated with white crosses) displayed in a Transverse (top left), Sagittal (bottom) and Coronal (top right) template brain section in one exemplary subject. POs= parieto-occipital sulcus. B) Top (left) and lateral (right) view of the target arrangement in the experimental task. The participants performed reaching movements with their right hand towards one of the nine targets (gray dots) located at different depths (far, intermediate and near) and in different directions (left, center and right). Reaching movements were performed in a darkened room from the initial hand position located next to the body (Home button), indicated by a square. C) Top view of the three task configurations. Top panel, Constant gaze configuration: reaching movements were performed towards one of the nine targets (hands). The spatial position of the target changed trial to trial, but the gaze was kept constant at the central position. Central panel, Constant reach configuration: reaching movements were always performed towards the target located in the central position. During the execution of the task, participants had to fixate one of the nine different positions (eyes). Bottom panel, Foveal reach configuration: reaching movements were performed towards one of the nine targets. During the task, the participant fixated and reached the same target (eye and hand on the panel). D) Time sequence of visually-guided reaching (only Constant gaze configuration is shown for conciseness). The small eye depicted in the figure represents the fixation point; the filled black dot represents the reaching target. The fixation point (a green point on the touchscreen) stayed on for 1.3 or 1.5 s and then the reaching target (a red point on the touchscreen) was turned on in one of the locations. Immediately, the participant had to reach with her/his right hand the visible position of the target while maintaining fixation on the fixation target (immediate reaching). During the reaction time, spTMS was delivered after 100 ms (100ms-trial) or 200 ms (200ms-trial). The fixation and the reaching targets were visible until the participant completed the movement. E) Sketch of the measurements of the precision and the accuracy of the reaching movements. An exemplary 95% confidence ellipse is shown, as well as the indication of depth and direction errors. 'Target' represents the reaching target.

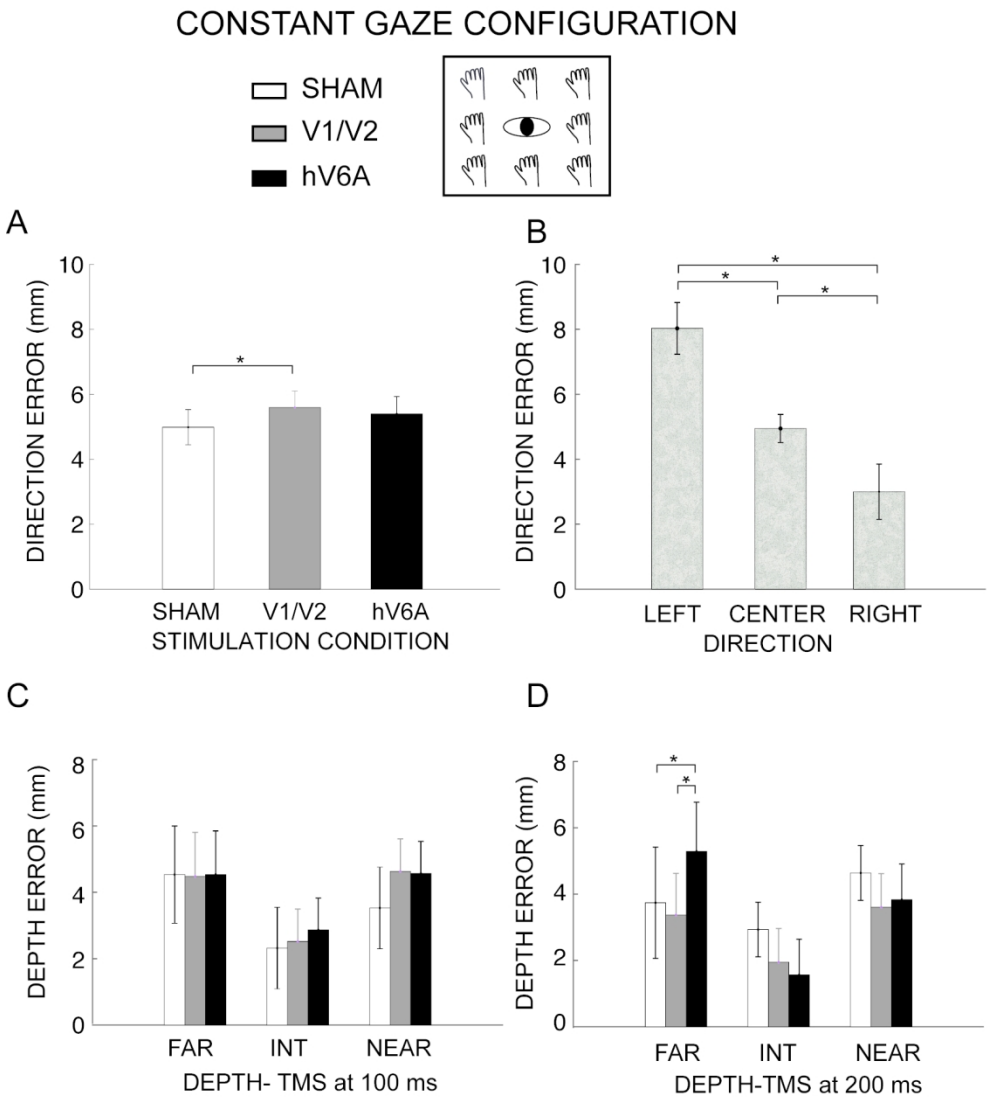

figure 2

Accuracy in the Constant gaze configuration. A) Distribution of direction errors in TMS delivered during Sham stimulation (SHAM, white), V1/V2 stimulation (V1/V2, dark gray) and hV6A stimulation (hV6A, black). A main effect of the Stimulation condition was evident, due to a decrease in accuracy after V1/V2 stimulation. B) Distribution of direction errors in the different directions of reaching. LEFT= left targets, INT=intermediate targets, RIGHT=right targets. Accuracy was influenced by the direction of reaching. C) Distribution of depth errors in the different stimulation conditions at different depths of reaching during 100-ms trials. No effect of TMS is shown. D) Distribution of depth errors in the different stimulation conditions at different depths of reaching during 200-ms trials. After spTMS over hV6A after 200 ms from the Go signal, reaching movements towards far targets were performed less accurately. FAR=reaching targets far from the body, INT=intermediate reaching targets, NEAR=reaching target near to the body. Asterisks indicate significant posthoc comparisons ($p<0.05$).

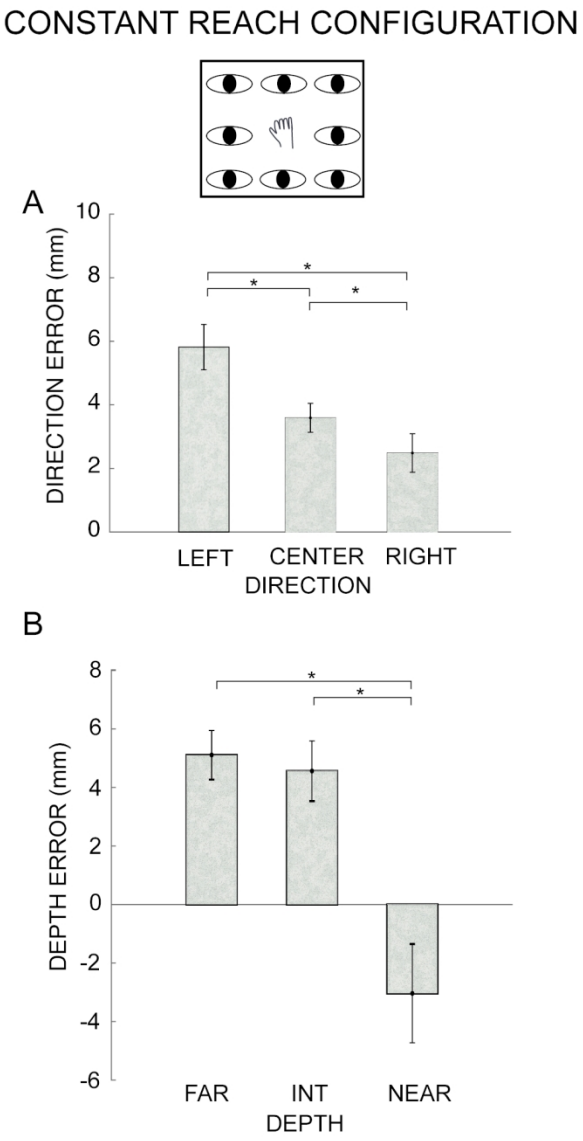

figure 3

Accuracy in the Constant reach configuration. A) Influence of the direction of the gaze position on direction errors, shown by the distribution of direction errors for reaching movements executed when the gaze was at different directions. Accuracy varied as a function of gaze position. B) Effect of depth of the gaze position on the depth errors, as shown by the distribution of depth errors for reaching movements executed when the gaze was at different depths (FAR=gaze positions far from the body, INT=intermediate gaze positions, NEAR=gaze positions near to the body). The depth of the gaze position influenced the reach accuracy. Other conventions as in figure 2.

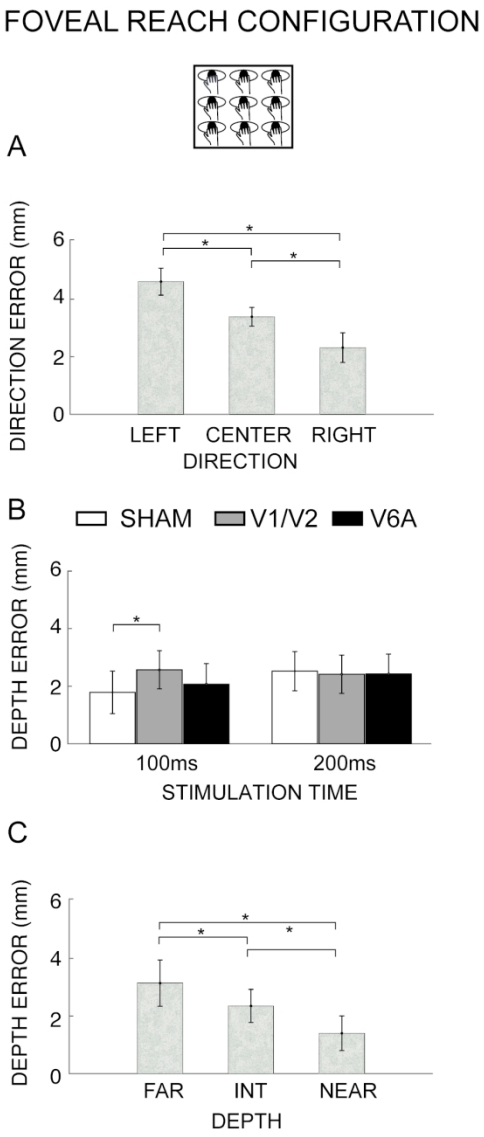

figure 4

Accuracy in the Foveal reach configuration. A) Effect of the direction of reaching on the direction errors, as shown by the distribution of direction errors for reaching movements executed toward targets located at different directions. The direction of foveal reaching influenced the reaching accuracy. B) Distribution of depth errors in 100-ms trials and in 200-ms trials in the different stimulation conditions. Stimulation of V1/V2 at 100 ms decreased the reaching accuracy. C) Effect of depth of reaching on the depth errors, as shown by the distribution of depth errors for reaching at different depths. Accuracy of reaching at different depths differed. Other conventions as in figure 2.

Supplementary material

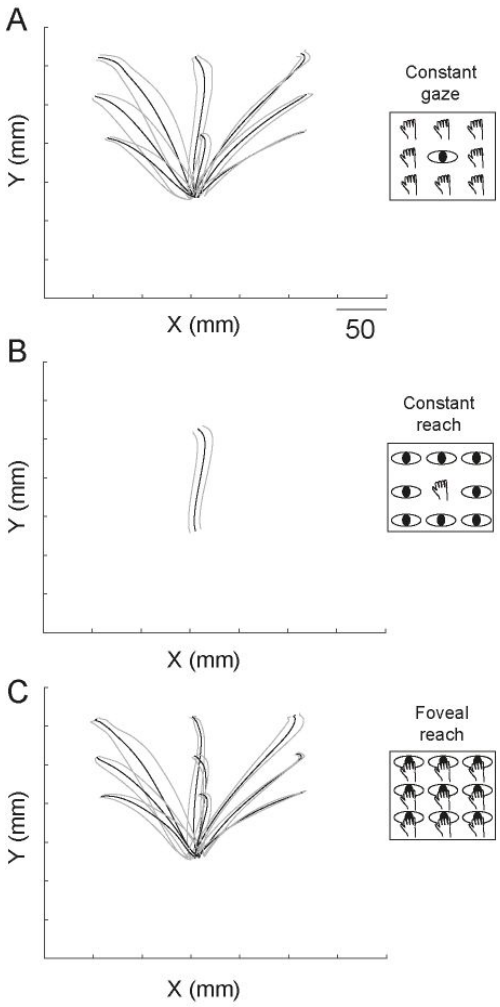

figure S1

Fig. S1

Actual trajectories of the reaching movement in the Sham condition. The trajectories of the index finger during movement in each of the three eye-hand configurations in one participant are shown. Black lines indicate the averaged trajectory and gray lines the X and Y variabilities along the movement.

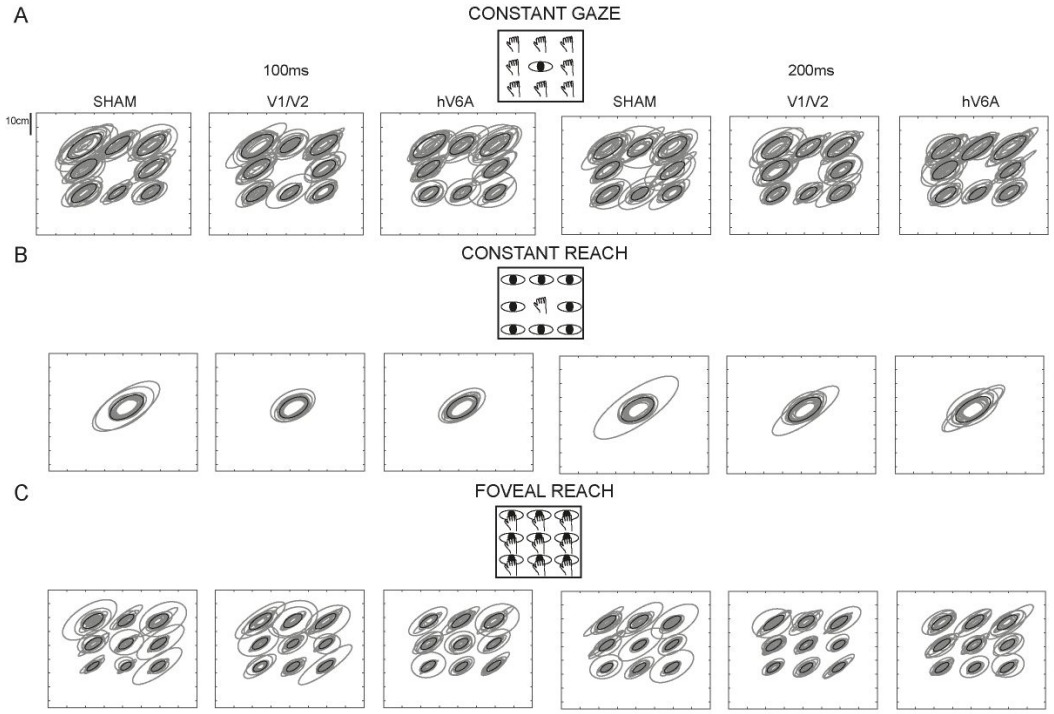

fig. S2

Fig. S2

Reaching precision in the different stimulation conditions.

A-C) Mean endpoint confidence ellipses for all 15 subjects (gray circles) and mean ellipses across all the subjects (black circles) during the visually-guided immediate reaching task in each of the 3 eye-hand configurations (top: Constant gaze; middle: Constant reach; bottom: Foveal reach). in 100-ms trials (left). in 200-ms trials (right). and in each of the 3 stimulation conditions (Sham. left. V1/V2. middle. hV6A. right. respectively). Horizontal and vertical axes correspond to the x- and y-coordinates in the horizontal plane. Despite the huge effects of depth and direction. no effect of spTMS on hV6A were found.

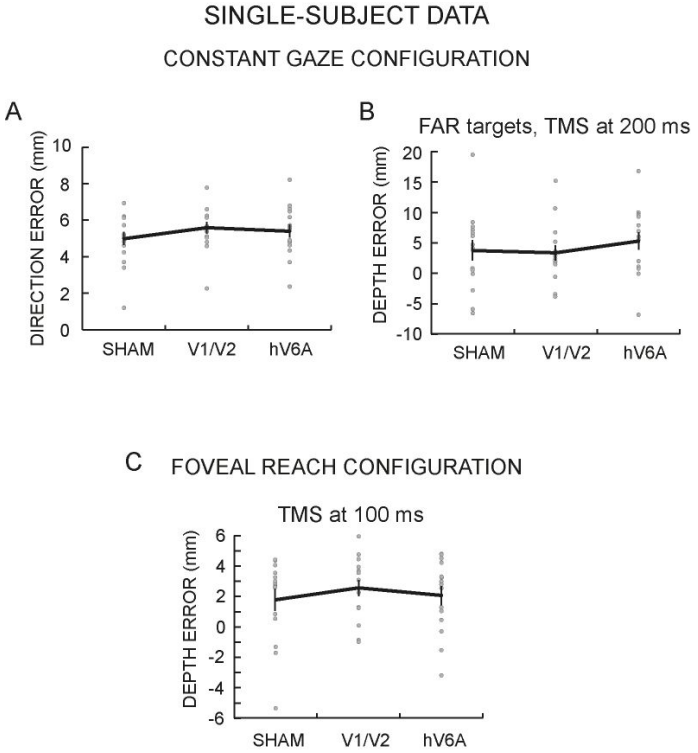

figure S3

Fig. S3

Single subject data

A) Direction errors of single subjects (grey dots) and mean value with SE (black line) in TMS delivered during Sham stimulation (SHAM), V1/V2 stimulation (V1/V2), and hV6A stimulation (hV6A) in the constant gaze configuration. B) Depth errors of single subjects (grey dots) and mean value with SE (black line) in TMS delivered during Sham stimulation (SHAM), V1/V2 stimulation (V1/V2), and hV6A stimulation (hV6A) in the constant gaze configuration for reaching towards far targets and TMS delivered after 200 ms of reaction time. C) Depth errors of single subjects (grey dots) and mean value with SE (black line) in TMS delivered during Sham stimulation (SHAM), V1/V2 stimulation (V1/V2), and hV6A stimulation (hV6A) in the foveal reach configuration with TMS delivered after 100 ms of reaction time.

Reach end-point precision

Constant gaze configuration (peripheral reaching)

Reach end-point precision was measured as the area of 95% confidence ellipses of the scatter of the fingertip at movement end (see Materials and Methods) (Fig. 1E). Figure S2A shows the ellipses of all the subjects (gray). and the mean ellipse (black) for the Constant gaze configuration.

We found that stimulation of hV6A did not influence the end-point precision in the constant gaze configuration (main effect of Stimulation Condition or interaction of the other factors by Stimulation Condition. all $F < 1.65$. all $p > 0.17$. all partial $\eta^2 < 0.1$). in agreement with previous studies of repetitive TMS delivered on the medial parietal cortex (Vesia et al. 2010), namely SPOC (Cavina-Pratesi et al. 2010) and on a more anterior parietal region (Marigold et al. 2019) homologue of monkey areas PEc/PE (Pitzalis et al. 2019).

As evident in the figure, a significant main effect of Depth ($F_{(2.28)} = 30.95$; $p < 0.001$. partial $\eta^2 = 0.69$) was found. Post hoc tests revealed that the precision during reaches towards farthest targets (9.88 mm^2 +/- 1.14) was lower than the one for reaches towards intermediate (6.64 mm^2 +/- 0.76) and near targets (5.65 mm^2 +/ -0.78. all $p < 0.001$. Fig. S2A). which in turn did not differ from one another ($p = 0.09$).

We also found a significant main effect of Direction ($F_{(2.28)} = 32.12$. $p < 0.001$. partial $\eta^2 = 0.69$) with reaches towards intermediate targets (4.46 mm^2 +/ -0.64) having the highest precision (right = 6.71 mm^2 +/- 0.82; left = 7.75 mm^2 +/ -0.9. $p < 0.001$ intermediate vs right and intermediate vs left. $p = 0.02$ right vs left).

Constant reach configuration (peripheral reaching)

A significant effect of Depth on precision was found ($F_{(2.28)} = 10.5$. $p < 0.001$. partial $\eta^2 = 0.42$): when gaze directed towards near targets (7.56 mm^2 +/- 0.77), reach was less precise than in the other configurations (far = 5.44mm^2 +/- 0.82; intermediate = 5.93 mm^2 +/- 0.68. near vs far and near vs intermediate $p = 0.002$; far vs intermediate $p = 0.32$).

We also found a significant main effect of Direction ($F_{(2.28)} = 33.2$. $p < 0.001$. partial $\eta^2 = 0.70$) with reaches towards central targets (4.01 mm^2 +/- 0.54) showing the highest precision (right = 9.10mm^2 +/- 1.08; left = 6.99 mm^2 +/- 1.05. $p < 0.001$ center vs right and center vs left. $p = 0.002$ right vs left).

Foveal reach configuration (foveal reaching)

A significant main effect of Depth (Figure S2C. $F_{(2.28)} = 12.4$. $p < 0.001$. partial $\eta^2 = 0.47$) was found. Similarly to the Constant gaze configuration. precision during foveal reaching towards farthest targets (4.67 mm^2 +/- 1.15) was lower than the one for reaching towards intermediate (2.69 mm^2 +/- 0.56) and near targets (2.35 mm^2 +/- 0.56. $p < 0.001$), which in turn did not differ from one another ($p = 0.49$).

No significant effects of Direction were found . all $F < 0.82$. all $p > 0.24$. all partial $\eta^2 < 0.09$.

Table S1

Mean values and standard errors of the reaction time and movement time of participants in different stimulation conditions (S = sham. hV6A = hV6A. V1/V2 = V1/V2). at different times (100ms. 200ms) and at different target depths (F = far. I = intermediate. N = near) of the Constant gaze configuration. RT = reaction time; MT = movement time; SE = Standard Error.

Stimulation condition	Stimulation Time	Depth	RT mean (ms)	RT SE	MT mean (ms)	MT SE
S	100	F	414.13	21.61	837.74	74.12
S	100	I	429.83	31.61	719.64	60.17
S	100	N	385.75	20.21	647.57	60.76
S	200	F	420.01	20.04	844.40	73.10
S	200	I	419.24	24.51	733.72	60.76
S	200	N	391.83	19.40	633.55	52.20
V1/V2	100	F	396.11	19.89	824.83	63.36
V1/V2	100	I	398.82	23.49	727.37	62.40
V1/V2	100	N	389.72	25.31	618.77	45.26
V1/V2	200	F	413.41	19.81	827.25	67.14
V1/V2	200	I	407.07	19.68	731.16	61.50
V1/V2	200	N	398.12	21.83	618.54	48.83
hV6A	100	F	432.11	33.80	840.52	67.56
hV6A	100	I	410.29	25.09	732.69	59.65
hV6A	100	N	384.38	20.82	626.34	45.43
hV6A	200	F	424.24	20.53	815.46	65.70
hV6A	200	I	424.12	24.12	726.36	56.78
hV6A	200	N	389.02	19.50	629.74	46.88

References

Cavina-Pratesi C. Monaco S. Fattori P. Galletti C. McAdam TD. Quinlan DJ. Goodale MA. Culham JC. 2010. Functional magnetic resonance imaging reveals the neural substrates of arm transport and grip formation in reach-to-grasp actions in humans. J Neurosci. 30:10306–10323.

Marigold DS. Lajoie K. Heed T. 2019. No effect of triple-pulse TMS medial to intraparietal sulcus on online correction for target perturbations during goal-directed hand and foot reaches. PLoS One. 14:e0223986.

Pitzalis S. Serra C. Sulpizio V. Di Marco S. Fattori P. Galati G. Galletti C. 2019. A putative human homologue of the macaque area PEc. Neuroimage.

Vesia M. Prime SL. Yan X. Sergio LE. Crawford JD. 2010. Specificity of human parietal saccade and reach regions during transcranial magnetic stimulation. J Neurosci. 30:13053–13065.